

Edge flow and radiation in Helium discharges in RFX

G. De Masi, M. Agostini, F. Auriemma, R. Cavazzana, E. Martines, B. Momo,
P. Scarin, M. Spolaore, G. Spizzo, N. Vianello and M. Zuin
Consorzio RFX, Euratom-ENEA Association, Padova, Italy

Introduction

RFX-mod is a Reversed Field Pinch toroidal device with $r/a = 2\text{m}/0.5\text{m}$. The best performance in terms of confinement properties is presently obtained at high plasma current ($I_p > 1.2$ MA) and medium-low electron density ($n_e/n_G \lesssim 0.3$, with $n_G = I_p/\pi a^2$ the Greenwald density) [1]. In this condition the plasma core gets globally self-organized in a rotating helical structure (Quasi Single Helicity state), characterized by the presence of one dominant tearing mode, strongly affecting also the edge plasma properties [2,3]. High density operations are instead limited by the superposition of a wide spectrum of $m=1$ MHD modes (Multiple Helicity, MH) producing magnetic field lines stochasticization in the plasma core and an increased Plasma Wall Interaction (PWI). An upper density limit has been found [4,5] for hydrogen operations (according to the Greenwald law) leading to a soft landing of the discharge due to excessive plasma resistivity. This limit has been explained in terms of a complex interaction between magnetic topology, radial electric field and edge flow rather than a simple PWI process. In particular, in [5] the role of the chain of poloidally symmetric magnetic islands (arising at the edge due to the presence of a $q=0$ surface) has been pointed as responsible for flow reversal and edge density accumulation in a toroidal localized region, with a phenomenology much similar to the Tokamak MARFE.

Since in RFX-mod plasma density is usually sustained by the hydrogen particles delivered by the carbon first wall (featuring a very high recycling), an unambiguous distinction of a cause and effect relation between PWI and density limit is not always possible. To this purpose, in this paper an analysis based on the high density helium discharges is presented. Helium does not show a chemical interaction with the carbon wall and, in principle, should allow the study of the edge phenomena properly belonging the RFP magnetic configuration.

Experimental results

In a set of reproducible helium discharges electron density has been raised up to $n_e/n_G \approx 0.8$ in a controlled way, until the increased plasma resistivity is so large that plasma current decays despite sustainment (the so called soft landing [4]). At this point, enhanced radiated power

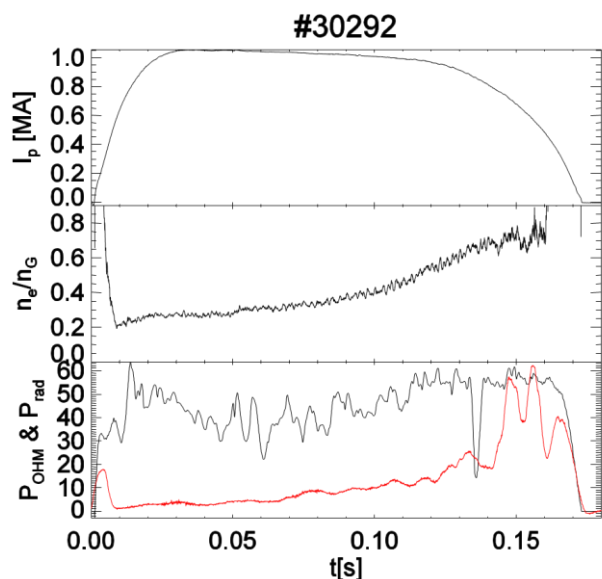


Fig. 1: Time evolution of plasma current (up), electron density normalized to the Greenwald one (middle) and of input power (black) compared to the radiated power (red) for a helium discharge.

flow is obtained by an Integrated System of Internal Sensors (ISIS) [2]. A reconstruction of the magnetic topology (based on the external magnetic measurements) in the (r, Φ) plane, is provided by the FLiT code solving the Newcomb's equations [6].

As already mentioned, due to the superposition and the phase locking (locked modes, LM) of a wide spectrum of $m=1$ MHD tearing modes (Multiple Helicity), $n_e/n_G \geq 0.35$ discharges are characterized by a strong PWI localized at the toroidal position Φ_{lock} in which the Last Closed Flux Surface intercepts the first wall (fig. 2). In this analysis, where possible the measured plasma parameters are referred to the instantaneous LM toroidal position Φ_{lock} . Moreover, the

poloidally symmetric $m=0$ island chain at the edge (present in all the RFP regimes) is toroidally modulated by the inner $m=1$ deformation. The result is a funnel-like structure ($m=0, n=1$) in which a part of the islands are pushed outwards intercepting the first wall (O-

P_{rad} (due to plasma cooling) equals the ohmic input power P_{OHM} (see an example in fig.1).

The analysis of the associated PWI and radiation pattern is based on a rich diagnostic equipment: a multichord interferometer (located at the toroidal angle $\Phi = 22.5^\circ$) provides the density profiles, particle influxes from the wall are estimated by H_α and He_I line emission measurements ($\Phi = 172.5^\circ$ and $\Phi = 82.5^\circ$ respectively) and the plasma radiation is monitored by a bolometric tomography ($\Phi = 202.5^\circ$). A toroidal map of the edge toroidal plasma

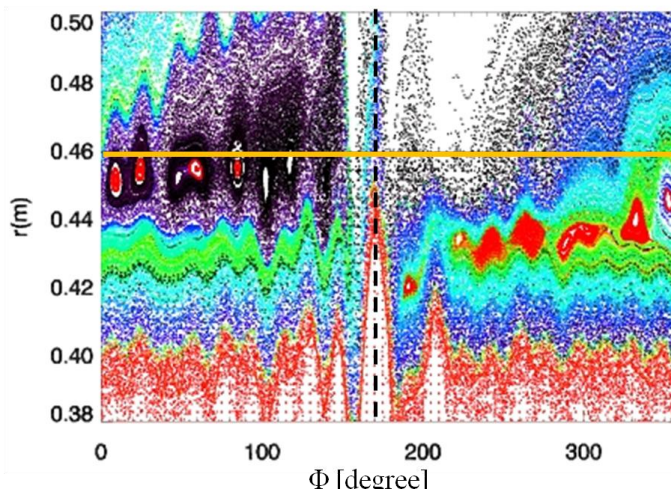


Fig. 2: #30292, $t = 0.140$ s. Poincaré plot in the (r, Φ) plane of the edge region for a typical MH magnetic topology. Field lines that do not intercept the first wall are coloured in red: among us the inner structure represents the Last Closed Field Surface and the outermost detached surfaces are $m=0$ islands. Dashed line indicates the toroidal position of the LM (Φ_{lock}) and the orange continuous line marks the first wall radial position.

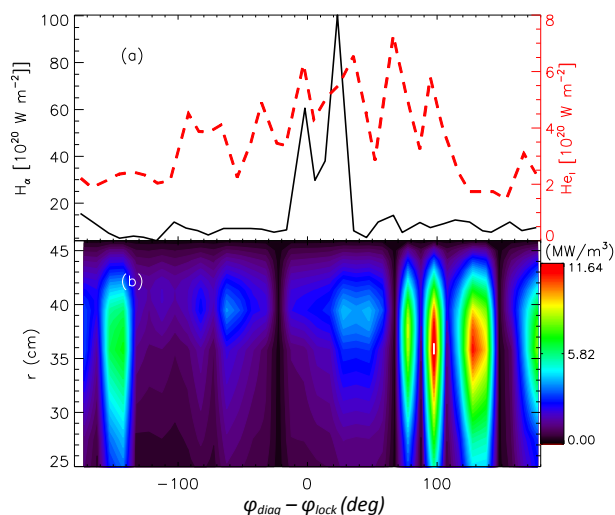


Fig. 3: #30292. (a) toroidal map of the H_α and the HeI influxes and (b) of total emissivity in the edge region.

Both the quantities are plotted with respect to the relative LM instantaneous position.

reflecting the fundamentally different nature of the PWI among the two species. Neutral particles enters the plasma at the LM position but they are conveyed to a broad region roughly located 100° toroidally far. Due to the local plasma cooling in that region, thus, a highly radiative layer takes place at the plasma edge (as shown in fig.3b). While, this behaviour is exactly the same found in pure hydrogen discharges [5], indicating that, even in the helium discharges considered here, the H influx affects the mechanism limiting the density, a smaller radiative region is found also at the position $\Phi_{diag} - \Phi_{lock}(t) \approx -150^\circ$.

Density profile, shown in fig. 4, almost flat in the first part of the discharge, becomes markedly hollow (the edge density reaching a value three times larger than the plasma core) when $\Phi_{diag} - \Phi_{lock}(t) \approx -150^\circ$, i.e., density

accumulation appears clearly related to a specific position with respect to the LM (fig. 4 upper plot). Unfortunately in its rotation, with respect to the interferometer location, the LM does not cover the position $\Phi_{diag} - \Phi_{lock}(t) \approx 100^\circ$ (where most of the radiation is concentrated).

A further modification of the edge plasma dynamics concerns the plasma flow. Low density

point) and part are detached from the wall (X-point) [5].

In the example shown in fig.3a, the H_α line emission measurement (solid curve) confirms the strong toroidal asymmetry of the PWI pattern (a non-negligible influx of hydrogen particles stored into the carbon wall is present also in helium discharges) localized in a narrow layer corresponding to the plasma column deformation due to the LM. On the other side, helium influx (fig.3a, dashed line) appears to be more uniform along the toroidal angle probably

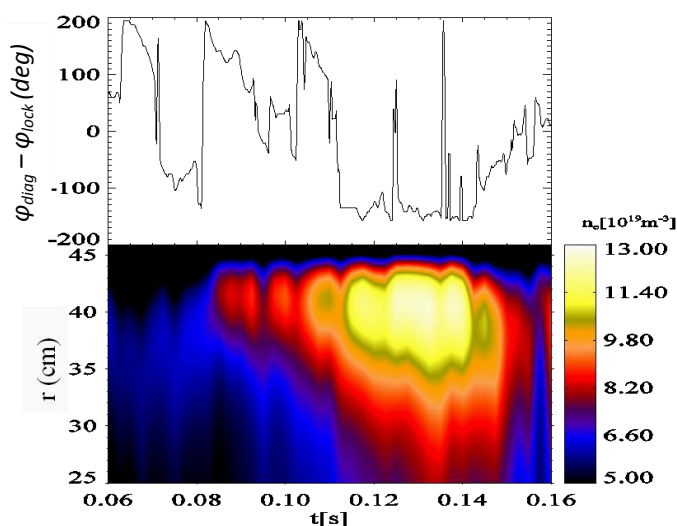


Fig. 4: #30292. Time evolution of the LM position with respect to the interferometer one (up) and contour plot of the edge density (down). Density accumulation appears linked to a specific relative distance from the LM position.

high plasma current regimes are characterized by a mainly helical flow pattern associated to the QSH 3D geometry [2]. At high density values instead, the toroidal map of the flow (fig. 5)

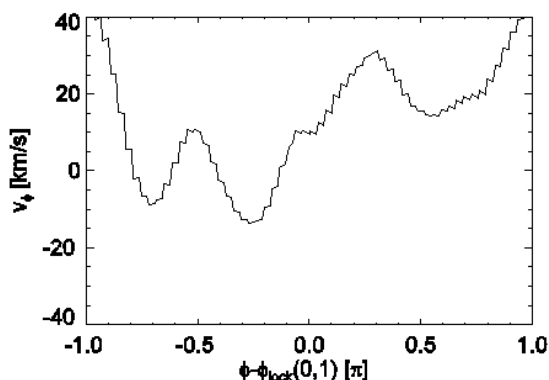


Fig. 5: #30292. Toroidal map of the edge toroidal flow at $t = 0.140$ s as a function of the relative distance to the LM instantaneous position.

appears strongly modulated by the $m=0, n=1$ structure created by the non-linear interaction between $m=1$ and $m=0$ modes. In particular, with the increasing density, the flow pattern becomes more complex and different regions with reversed positive flow arise at the edge.

Discussion

High density RFP regimes with helium as a filling gas show similarities and differences with respect to the hydrogen case. The picture based on a source-stagnation point mechanism previously proposed [4,5] seems largely fitting also the experimental observations presented in this paper. While the hydrogen particle influxes (fig. 3a) are clearly associated to the LM position (the source), helium influx behaviour appears more uniform along the toroidal direction (covering a 200° degree wide region around the position $\Phi_{diag} = \Phi_{lock}$). Even more important is probably the behaviour of density and radiation. In the helium case two stagnation points are observed: density accumulates around the position $\Phi_{diag} - \Phi_{lock} \approx -150^\circ$ (fig.4), while radiation shows a larger peak around the position $\Phi_{diag} - \Phi_{lock} \approx 100^\circ$ and a smaller one at $\Phi_{diag} - \Phi_{lock} \approx -150^\circ$ (fig. 3). Since in the considered experiments the LM position do not cover in its rotation all the toroidal positions (fig. 4 upper plot), from these experimental observations one could just suppose that a uniform broad stagnation point takes place between the two diagnosed toroidal positions. The mechanism producing this picture would be driven by the edge toroidal flow. In the high density hydrogen regimes a single flow reversal region had been associated to a convective cell generated by a parent ($m=0, n=1$) island [5]. In this case, instead, also the magnetic topology is slightly different since well conserved $m=0$ flux surfaces are distributed in a broader toroidal region (red filled surfaces in fig. 2). That would cause toroidal flow to reverse in different points (fig. 5) as density increases and thus density and radiation to stagnate in a larger region with respect to the hydrogen case. As a final remark, it is worth mentioning that even in helium discharges the ratio between helium and hydrogen influxes is never above 0.5 (0.25 for this pulse) so that the global edge dynamics is the result of a superposition of edge phenomena.

This work was supported by the European Communities under the contract of Association between EURATOM/ENEA. The views and opinions expressed herein do not necessarily reflect those of European Commission

- [1] P. Martin et al., Nucl. Fusion **51**, (2011) 094023;
- [2] P. Scarin et al., Nucl. Fusion **51**, (2011) 073002
- [3] G. De Masi et al., Nucl. Fusion **51**, (2011) 053016
- [4] M. E. Puiatti et al., Nucl. Fusion **49**, (2009) 045012
- [5] G. Spizzo et al., Plasma Phys. Control. Fusion **52**, (2010) 095011
- [6] P. Innocente et al., Nucl. Fusion, **47** (2007) 1092